Japanese Journal of Applied Physics **50** (2011) 10PF05 **REGULAR PAPER**
DOI: 10.1143/JJAP.50.10PF05

Semi-Analytical Depletion Width Evaluated by Self-Consistent Schrödinger–Poisson Pair Calculations

Che-Sheng Chung*

Department of Electronic Engineering, National Taiwan University of Science and Technology, Taipei 106, Taiwan, Republic of China

Received January 29, 2011; accepted July 25, 2011; published online October 20, 2011

A self-consistent calculation establishes a bulk built-in potential by applying a DC bias to a gate/insulators/semiconductor (GIS) structure of a metal–oxide–semiconductor field-effect transistor (MOSFET). The width of a semi-analytical depletion layer near the interface of the GIS structure of an n-type MOSFET (nMOSFET) can be extracted by self-consistent calculation. The grand canonical ensemble improves the quantitative calculation for the theoretical evaluation of the self-consistent calculation. It is possible that a new approximation establishing the self-consistent potential appropriately merges with a classical transport model at low temperatures because of minimizing quantum calculations in a momentum space. © 2011 The Japan Society of Applied Physics

1. Introduction

In 1972, Dr. Frank Stern and his IBM colleagues announced that they had triumphed over approaching a long range self-consistent potential by a triangular potential approximation theoretically.[1,2] Since a self-consistent Schrödinger–Poisson pair calculation is promising for predicting quantum features of a long range micron- or nano-tissue in modeling a metal–oxide–semiconductor field-effect transistor (MOSFET) at low temperatures, an off-current can be characterized by a no-noise self-consistent potential of *ab initio* calculations.[3–9] However, until now, the self-consistent potential has not been used in evaluating the low leakage current or the off-current of a conventional drift-diffusion model.

By considering a theoretical derivation of eliminating pinning effects at an interface of a gate/insulators/semiconductor (GIS) structure and ignoring the non-uniformity of a doped substrate, a no-noise self-consistent calculation can produce charge centers near the interface of the GIS structure.[6] By applying a DC gate bias to the GIS structure at low temperatures ($\geq$77°K), Fig. 1 shows a built-in surface potential formed at the bulk of an n-type MOSFET (nMOSFET) near the flatband mode. The self-consistent calculation establishes a built-in surface potential, $V(z)$, possessing a semi-analytical depletion layer width, $W(V)$, extracted by a semi-analytical approach combining with the use of analytical derivations and of numerical iterations.[4,10] Because the self-consistent calculation dynamically refreshes the depletion width with respect to the iteration routine, which follows a numerical iteration of recursive algorithms, the semi-analytical depletion width is also called the dynamic depletion width in this work.[10] That is, dynamically extracting a depletion layer width is a procedure of numerically stimulating a semi-analytical approach. A semi-analytical approach assists in understanding the calculation of a semi-analytical depletion width in detail.[4,10]

During the period time of relaxing the self-consistent calculation, a problem was discovered in the calculations of the carrier distributions. If a self-consistent calculation based on a semi-classical approximation is valid, calculating a carrier population counts on not only the number of calculated carriers in a momentum space but also the quantum transform transferring a quantum wave from a momentum space to a real space. Usually, observing a local carrier momentum in a momentum space is difficult. Quantum evidence in a momentum space weakly appear or do not appear on the data measured by electrical instruments at low temperatures.[11,12] The impacts of discrete distribution functions generated by the calculations of mobile charges can not apparently appear on the results of the self-consistent calculations at low temperatures.

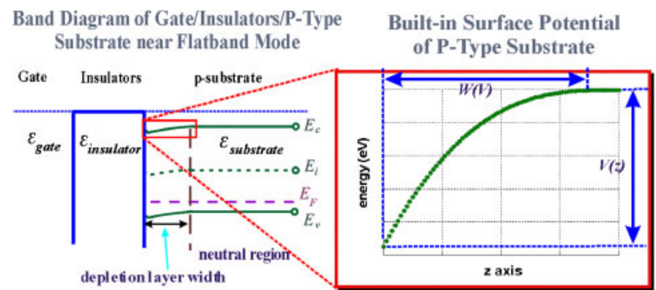

Fig. 1. (Color online) Built-in surface potential $V(z)$ and semi-analytical depletion width $W(V)$ of a GIS structure near flatband mode.

Secondly, a potential energy, which recursively feeds to a Schrödinger's equation, from the calculation of Poisson's equation complicatedly nests a recursive structure in calculating the quantum wave of a carrier. In addition, for having a fast and stable solution, simplified quantum calculations of the self-consistent calculation are in use. In considering a one-particle case in a mesoscopic system, a new approximation minimizing quantum calculations in a momentum space is a better interpretation than a conventionally semi-classical approximation at low temperatures. This paper proposes an example of numerically extracting the width of semi-analytical depletion layer per built-in potential by the self-consistent calculation based on the new approximation.

To document the new approximation and to distinguish it from a semi-classical approximation analytically, an *r*-space of which a phrase is originally an abbreviation of a real space replaces a real space. That is, the new approximation defines subband energies in an *r*-space and a semi-classical approximation has real space or momentum space subband energies in a mesoscopic system. Since an approximation is close to the classical theory in an *r*-space, most of the quantum effects, e.g., the interactions of quantum carriers and quantum Fourier transforms, are not valid in a self-

*E-mail address: chungten@ms81.hinet.net

 © 2011 The Japan Society of Applied Physics

consistent calculation except for simplified quantum calculations.[10] On the contrary, if a semi-classical approximation is valid in a real space, quantum calculations in a momentum space are suitable for self-consistent calculations.[3–9,11,12] For simplicity, the quantum calculations of the new approximation, for the first time, only involve the numbers of momentum space quantum carriers, r-space quantum waves, and the r-space subband energies.[10] Obviously, the new approximation proposed to fill a gap bridging the classical and semi-classical theories is not treated as a semi-classical approximation. According to the published lines of evidence obtained by electrical instruments at low temperatures, the proposed approximation resolves the ambiguous conflicts from the semi-classical theory in a mesoscopic system.[11,12]

2. Theoretical Calculations

A semi-analytical approach provides an understanding of the self-consistent calculation based on a potential approximation. Similarly to that observed for a semi-classical approximation, Schrödinger's equation and Poisson's equation of the self-consistent calculation are also the main equations of the proposed approximation. If assuming that chemical solubility is at saturated, a Hamiltonian operator, $\tilde{H}$, of a one-dimensional (1D) Schrödinger's equation is given by[1,2,13]

$$\tilde{H}\zeta_{ij}(z) = \left[\frac{p_{ij}^2}{2m_z} + V(z)\right]\zeta_{ij}(z) = E''_{ij}\zeta_{ij}(z), \quad (1)$$

where $V(z) \equiv q\psi_s(z)$ denotes the potential energy and $\psi_s(z)$ is the built-in surface potential. $\zeta_{ij}(z)$ and p_{ij} are the 1D normalized wave function and the carrier momentum at the ith subband of the jth valley, respectively. E''_{ij} is the double prime eigen energy. m_z is the effective mass of carriers in the z direction.[13] For simplicity, a 1D Poisson's equation for a p-type semiconductor tissue is given by

$$\frac{d^2\psi_s(z)}{dz^2} = -\frac{[\rho_{\text{ions}}(z) + \rho_h(z) + \rho_e(z)]}{\varepsilon_{\text{Si}}}, \quad (2)$$

where ε_{Si} is the dielectric constant of silicon. $\rho_{\text{ions}}(z)$, $\rho_h(z)$, and $\rho_e(z)$ are the charge sheet densities of ions, of holes, and of electrons induced, respectively.[14]

$$\rho_{\text{ions}}(z) \equiv -[eN_D^+(z) - eN_A^-(z)], \quad (2a)$$

$$\rho_h(z) \equiv -ep_p(z), \quad (2b)$$

$$\rho_e(z) \equiv en_p(z). \quad (2c)$$

The charge sheet densities lead to the calculation of the electric field. By considering the conventional derivation of Kingston's equation to deal with charge sheet densities associated with a 1D Poisson's equation, the equivalent electric field of a p-type semiconductor approximates[1,15)]

$$\Xi_S^2 - \Xi_B^2 = \frac{-2\left[\int_{\psi_{s0}}^{\psi_{s\infty}} \rho_{\text{ions}}\, d\psi_s + \int_{\psi_{s0}}^{\psi_{s\infty}} \rho_h\, d\psi_s + \int_{\psi_{s0}}^{\psi_{s\infty}} \rho_e\, d\psi_s\right]}{\varepsilon_{\text{Si}}}, \quad (3)$$

where Ξ_S is the total electric field for bound states and Ξ_B is the electric field at the bulk end. $\psi_{s\infty}$ and ψ_{s0} are the built-in surface potentials at the bulk and interface ends, respectively. Because the electric field calculated is usually below 0.1 V/cm, the mobility impacting on the transport of quantum carriers within a built-in potential is ignored for bound states.[11,16] That is, the self-consistent calculation in this case does not involve some minor effects of the proposed approximation.

3. Carrier Concentrations and Discrete Subbands

After considering the thermal impacts affecting carriers, we assume that a free electron for bound states flies over the Fermi surfaces at bulk. That is, the proposed approximation only calculates the number of low temperature quantum carriers in a momentum space. For simplicity, by considering the suggestion of Stern and Howard, the density of electrons induced in a p-type semiconductor approximates[1]

$$n_p = \left(\frac{g_A k_B T m_z}{\pi\hbar^2}\right) \times \sum_{j=1}^{m}\sum_{i=0}^{n} \zeta_{ij}(z)\left\{\frac{\ln[1+\exp(\eta_{Fp} - u_s)]}{\ln[1+\exp(\eta_{Fp} - \eta_c)]}\right\}\zeta_{ij}^*(z), \quad (4)$$

where $\zeta_{ij}^*(z)$ is the complex conjugate of a quantum wave, $\zeta_{ij}(z)$. m and n are the maximum numbers of valleys and subbands, respectively. $m_z = \sqrt{m_t m_l}$. m_l is the effective mass of electrons induced at the horizontal orientation of the z-axis and m_t is the effective mass of electrons induced at the vertical orientation of the z-axis. g_A is the degenerate factor of holes. k_B is the Boltzmann constant and T is the temperature. $u_s = [E''_{ij} - V(z)]/k_B T$, $\eta_{Fp} = E_{Fp}/k_B T$, and $\eta_c = E_c/k_B T$ are the reduced carrier energy, the reduced Fermi energy level of a p-type substrate, and the reduced edge energy of a conduction band, respectively. $\hbar$ is the reduced Planck constant.

On the basis of electron gas theories, as for the charge sheet densities, the Fermi–Dirac distribution functions and integrals represent the source functions of Poisson's equation in a p-type substrate. By considering the grand canonical ensemble of minority charge density within a unitary box of valence bands, the hole concentration of a p-type semiconductor approximates[6–9,11]

$$p_p = N_v\left(\frac{2}{\sqrt{\pi}}\right)\frac{\sum_{j=1}^{m}\sum_{i=0}^{n}\zeta_{ij}(z)F_\gamma[\eta_{Fp} - \eta_v - g_A u_s]\zeta_{ij}^*(z)}{\sum_{j=1}^{m}\sum_{i=0}^{n}\zeta_{ij}(z)\zeta_{ij}^*(z)}, \quad (5)$$

where $N_v = (1/4)(2m_h k_B T/\pi\hbar^2)^{3/2}$ is the effective density of states in the valence band if a parabolic valence band is valid. Moreover, $u_s = [E''_{ij} - V(z)]/k_B T$ and $\eta_v = E_v/k_B T$ are the reduced carrier energy and the reduced edge energy of a valence band, respectively. F_γ is the Fermi–Dirac integral representing a dispersion behavior of carriers at a specific temperature and γ is the subscript (e.g., $-1/2$ and $1/2$) of the Fermi–Dirac integral. The charge concentrations of carriers over an n-type semiconductor show the other set of similar equations.

The quantum part of the self-consistent calculation adjusts the double prime eigen energies and self-consistent potential energies.[17] On the basis of the grand canonical ensemble of quantum statistical mechanics, the total double prime eigen energy approximates[2,14]

© 2011 The Japan Society of Applied Physics

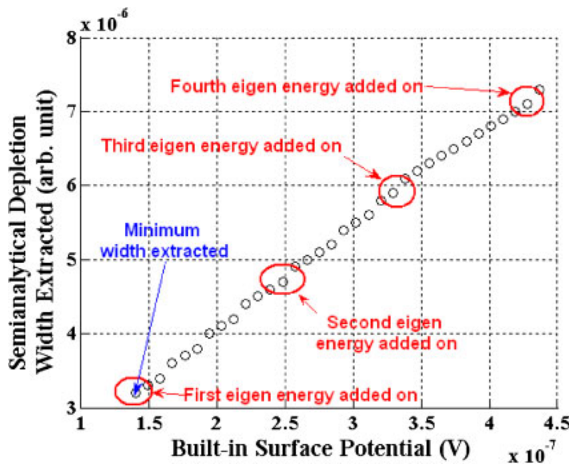

Fig. 2. (Color online) Almost linear relationship of semi-analytical depletion layer width (arbitrary unit or arb. unit) extracted vs built-in surface potential (V) based on the new approximation in this work.

$$\left\langle \sum_{j=1}^{m}\sum_{i=0}^{n} E_{ij}'' \right\rangle = \frac{\displaystyle\sum_{j=1}^{m}\sum_{i=0}^{n}\int_{0}^{\infty} \zeta_{ij}(z)\tilde{H}\zeta_{ij}^{*}(z)\,dz}{\displaystyle\sum_{j=1}^{m}\sum_{i=0}^{n}\int_{0}^{\infty} \zeta_{ij}(z)\zeta_{ij}^{*}(z)\,dz}. \quad (6)$$

A population of carriers sums up with the carriers of discrete subbands, although the distribution of carrier concentration is a continuous, smooth, and monotonic curve at temperatures above 77°K.[11,12)]

4. Results

To eliminate propagation errors in a self-consistent calculation, recursive iterations are considered in the calculation of a self-consistent potential.[10)] Several numerical algorithms for converging recursive iterations enable the calculation of the self-consistent potential by incorporating a set of semiconductor process parameters and numerical conditions while extracting a semi-analytical width automatically.[10)] As shown in Fig. 2, the self-consistent calculation can generate an almost linear curve of semi-analytical depletion width with respect to built-in surface potential in a range from 0.14 to 0.44 μV to a p-type semiconductor.

A minimum semi-analytical depletion width based on the approximation is valid if the first subband appears in the first calculation. In this case, on the basis of one-particle approximation, a minimum Debye length appears at about 3.2×10^{-6} arbitrary unit (arb. unit) while establishing a built-in surface potential, 0.14 μV, by an external DC bias.

I discovered that the numerical algorithms of the self-consistent calculation resulted in both the efficient coding of a program and improvement of the convergent rate of the self-consistent calculation.[10)] To shorten simulation times to satisfy electrical applications, the proposed approximation minimizes quantum calculations in a momentum space.

5. Discussion

The curve has several little ramps shown in Fig. 2. Although a self-consistent potential energy adds on an eigen energy by increasing the external DC bias to the GIS structure, a little ramp appears on the curve in Fig. 2. Because the self-consistent calculation involves several numerical algorithms leading to a stable calculation, a non linear error, which is a combination of truncation errors, rounding errors, etc., introduced by an algorithm impacts the scale of an extracted semi-analytical width.[10)] If a semi-analytical width at a specific point is extracted by a different algorithm, the unit of the extracted semi-analytical width is no longer on the same scale. That is, if the neighboring points involve different algorithms in extracting semi-analytical widths, a little ramp also usually appears on the curve in Fig. 2.

6. Conclusions

Although the program from IBM enables the calculation of an analytical depletion layer width, the self-consistent calculation demonstrates the solution to the numerical extraction of a semi-analytical depletion layer width in an r-space.[5,10)] Obviously, following a semi-analytical approach, the numerical Debye length can replace an analytical Debye length if the unit of numerical Debye length is determined.[10,18)]

The proposed approximation can support the self-consistent calculation associated with a drift-diffusion model for predicting the leakage current or off-current of a degenerate semiconductor by appropriately adjusting the fitting parameters of the self-consistent calculation.[10–12)]

Acknowledgments

The author would like to thank Professor Sheng-Lyang Jang of National Taiwan University of Science and Technology for leading me to his surface potential work and Professor Ying-Sheng Huang of National Taiwan University of Science and Technology for suggesting me in reading materials regarding low-level measurements.

1) F. Stern and W. E. Howard: Phys. Rev. **163** (1967) 816.
2) F. Stern: Phys. Rev. B **5** (1972) 4891.
3) S. Selberherr: IEEE Trans. Electron Devices **36** (1989) 1464.
4) E. Gnani, S. Reggiani, M. Rudan, and G. Baccarani: Proc. 34th ESSDERC, 2004, p. 177.
5) F. Rana, S. Tiwari, and D. Buchanan: Appl. Phys. Lett. **69** (1996) 1104.
6) S. A. Hareland, S. Krishnamurthy, C.-F. Yeap, K. Hasnat, A. F. Tasch, Jr., and C. M. Maziar: IEEE Trans. Electron Devices **43** (1996) 90.
7) S. V. Walstra and C.-T. Sah: IEEE Trans. Electron Devices **44** (1997) 1136.
8) T. Janik and B. Majkusiak: IEEE Trans. Electron Devices **45** (1998) 1263.
9) F. Assad, Z. Ren, D. Vasileska, S. Datta, and M. S. Lundstrom: IEEE Trans. Electron Devices **47** (2000) 232.
10) C.-S. Chung and S.-L. Jang: 4th IEEE INEC2011, 2011, G12-4, p. 34 (submitted to Solid-State Electron. Special Issue: INEC2011).
11) J. P. Colinge, A. J. Quinn, L. Floyd, G. Redmond, J. C. Alderman, W. Xiong, C. R. Cleavelin, T. Schulz, K. Schruefer, G. Knoblinger, and P. Patruno: IEEE Electron Device Lett. **27** (2006) 120.
12) F. Boeuf, X. Jehl, M. Sanquer, and T. Skotnicki: IEEE Trans. Nanotechnol. **2** (2003) 144.
13) T. Ando, A. B. Fowler, and F. Stern: Rev. Mod. Phys. **54** (1982) 437.
14) R. Seiwatz and M. Green: J. Appl. Phys. **29** (1958) 1034.
15) C. Moglestue: J. Appl. Phys. **59** (1986) 3175.
16) S. Takagi, T. Iisawa, T. Tezuka, T. Numata, S. Nakaharai, N. Hirashita, Y. Moriyama, K. Usuda, E. Toyoda, S. Dissanayake, M. Shichijo, R. Nakane, S. Sugahara, M. Takenaka, and N. Sugiyama: IEEE Trans. Electron Devices **55** (2008) 21.
17) Y. Ohkura: Solid-State Electron. **33** (1990) 1581.
18) D. Vasileska, S. S. Ahmed, and G. Klimeck: https://nanohub.org/resources/4443

© 2011 The Japan Society of Applied Physics